Technical Note

Separation Zone in Flow past a Spur Dyke on Rigid Bed Meandering Channel

Kedar Sharma[1] and Pranab K. Mohapatra[2]

Abstract: Flow past a spur dyke on a rigid bed meandering channel with a trapezoidal cross section has been studied experimentally. An acoustic Doppler velocimeter (ADV) was used to measure the velocities. The results show that length of the downstream separation zone changes according to the location of the spur dyke. It varies from 4.0 to 22.8 times the spur dyke length. In addition, the separation zone at higher elevations is wider compared to that near the bed for most of the locations of the spur dyke. The effect of contraction ratio and inflow Froude number on separation zone is also presented. **DOI: 10.1061/(ASCE)HY.1943-7900.0000586.**

CE Database subject headings: Meandering streams; Channels; River beds; Flow rates; Acoustic techniques.

Author keywords: Spur dyke; Meandering channel; Velocity field; Separation zone; Acoustic Doppler velocity meter.

Introduction

Spur dykes are used to protect the river banks from erosion and to deepen the main channel for creating a navigational channel. Characteristic parameters of a spur dike are dike length (b), height, width, shape, inclination to the downstream bank (α), and permeability. Separation zones are observed both on the upstream and downstream sides of a spur dike (Ettema and Muste 2004). As shown in Fig. 1, the downstream separation zone may be characterized by the downstream length (L_1), the maximum width (W_{max}), and the distance of maximum width from the spur dike (L_2). Corresponding nondimensional parameters (L_1^*, L_2^*, and W_{max}^*) may be obtained by using b as a scaling parameter. Contraction ratio (CR), is the ratio of spur dike length to channel width.

The flow field and flow separation zone due to a spur dike in a straight rectangular channel with rigid bed have been studied experimentally by various researchers (Rajaratnam and Nwachukawa 1983; Ettema and Muste 2004) and numerically (Tingsanchali and Maheswaran 1990; Molls and Chaudhry 1995; Ouillon and Dartus 1997) (see Table 1). In some recent numerical studies (Nagata et al. 2005; Koken and Constantinescu 2008; Koken 2011), the main emphasis was to analyze the flow field near a spur dike on a mobile bed. A few studies for flow past spur dike(s) in a meandering channel are also reported. Giri et al. (2004) measured the velocity field near spur dykes in a meandering laboratory flume. Details of the separation zone were not discussed in the previous study. The effect of location of the spur dike on L_1^* in a sine-generated channel with a trapezoidal cross section was presented by Sharma and Mohapatra (2009). They used the numerical model CCHE2D for flow field simulation and found that the maximum and minimum values of L_1^* were 16.6 and 3.1, respectively.

To the authors' knowledge, a detailed description of the separation zone for flow past a spur dike in a meandering channel is missing. Thus, the main objective of the present study is to present the mean velocity field and separation zone due to flow past a perpendicular spur dike in a rigid bed meandering channel.

Experimental Procedure

The experiment has been carried out in the Hydraulics Laboratory of the Indian Institute of Technology, Kanpur. The channel center line follows a sine-generated curve represented by $\theta = \theta_0 \cos(2\pi s/L)$ with $\theta_0 = 50^\circ$, the length of the sine-generated channel along the channel center line, $L = 6.2$ m, and the wave length, $\lambda = 4.65$ m (Fig. 2). A quarter portion of the curve is extended both on the upstream and on the downstream sides. The lengths of the straight reaches upstream and downstream sides are 2.5 and 1.5 m, respectively. The trapezoidal channel section is made up of cement mortar and has a bottom width of 0.52 m, side slope of 1:1, and height of 0.25 m. The channel bed is horizontal. Water from a constant head reservoir is supplied to the channel. A honeycomb is used at the upstream of the channel to ensure calm entrance of water. A tail gate is used at the downstream end of the channel to control the flow depth. The spur dike used in the present study is a wooden block with a height of 0.25 m and thickness of 0.03 m. Water surface measurements are performed by a point gauge with an accuracy of ±0.001 m. The three-dimensional velocity field is measured with the help of a downward-looking acoustic Doppler velocimeter (ADV) (Nortek 2011) attached to a traverse.

Any space in the channel is defined by a curvilinear coordinate system, i.e., s = along the center line of the flume; n = along lateral direction; and z = along vertical direction, with origin located on the bed at O (Fig. 2). The corresponding nondimensional coordinates are defined as $s^* = s/L$; $n^* = n/B$; and $z^* = z/H_{rep}$ where B = channel half width at half of the representative flow depth and H_{rep} = representative flow depth defined by the water surface measured at $s = -2.55$ m and $n = 0.0$ m. The resultant velocity is defined as $\bar{U} = \sqrt{\bar{u}^2 + \bar{v}^2}$. The recorded velocity in the vertical direction, w, is not used in this study. The discharge is estimated

[1]Research Scholar, Dept. of Civil Engineering, Indian Institute of Technology Kanpur, Kalyanpur, Kanpur, India-208016. E-mail: kedarsk@iitk.ac.in

[2]Associate Professor, Dept. of Civil Engineering, Indian Institute of Technology Kanpur, Kalyanpur, Kanpur, India-208016 (corresponding author). E-mail: pranab@iitk.ac.in

Note. This manuscript was submitted on December 4, 2010; approved on February 29, 2012; published online on March 3, 2012. Discussion period open until March 1, 2013; separate discussions must be submitted for individual papers. This technical note is part of the ***Journal of Hydraulic Engineering***, Vol. 138, No. 10, October 1, 2012. © ASCE, ISSN 0733-9429/2012/10-897-901/$25.00.

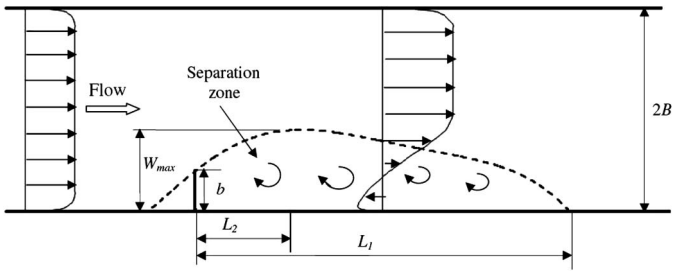

Fig. 1. Flow around spur dyke

Table 1. Parameters of Flow Separation Zone (Spur Dyke in Straight Channel)

Reference	Method	L_1^*	L_2^*	W_{max}^*
Rajaratnam and Nwachukawa 1983	Experimental	12		
Ettema and Muste 2004	Experimental	13–14		
Tingsanchali and Maheswaran 1990	Numerical	10–12	5.0	1.8
Ouillon and Dartus 1997	Numerical	10–12		

by the velocity area method. The velocity measured at $s = -2.55$ m, $n = 0.0$, and $z = 0.06$ m is the representative velocity, $\bar{U}_{rep}$, and is used to normalize the velocity. All velocity measurements are recorded for 120 s with a frequency of 25 Hz. It was verified by using different time windows that time averaging produces similar results when the time window is 60 s or higher. However, in the present study, 120 s is used for time averaging. The cross-section being trapezoidal, b is defined as the length at $z^* = 0.50$. The measurements are performed at two elevations, i.e., at $z^* = 0.167$ (0.02 m from bed) and $z^* = 0.50$ (0.06 m from bed) and in a grid with $\Delta s^* = 0.0208$ and $\Delta n^* = 0.156$. In this study, all output data from ADV were postprocessed by using a public domain software WinADV-version 2.027 (Wahl 2003). Data points having correlation scores less than 70% were rejected. The time averaged velocities, $\bar{u}$ and $\bar{v}$, obtained from the instantaneous velocities, u and v, are used in the analysis.

Results

The present study takes into account 24 different cases to evaluate the effects of spur dike location, spur dike length, and inflow Froude number on the velocity field and flow separation zones (Table 2).

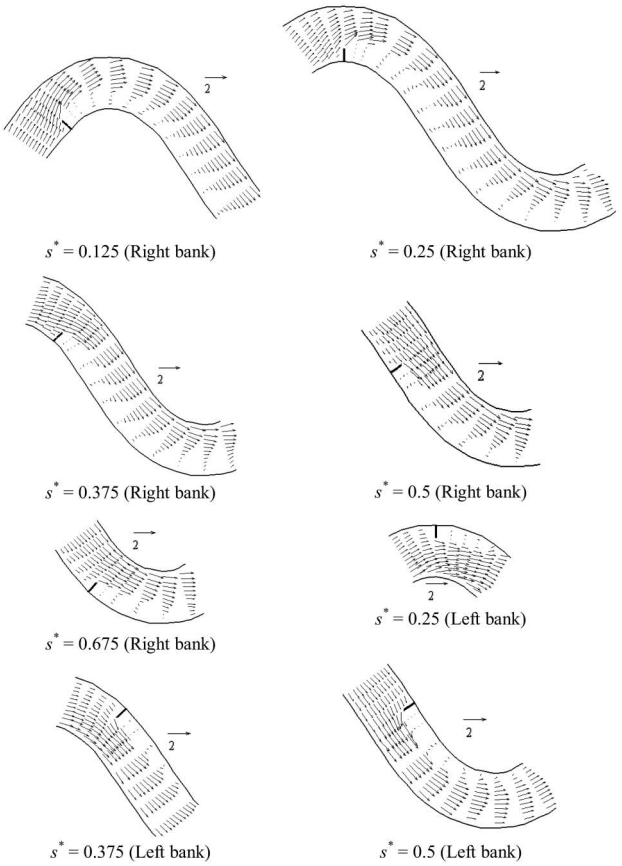

Fig. 3. Effect of spur dyke location on velocity field at $z^* = 0.5$

Mean Velocity

The mean velocity field at $z^* = 0.50$ for different locations of the spur dike is presented in Fig. 3. It also indicates the upstream and the downstream flow separation zones. The observed maximum value of $\bar{U}^*$ is 2.26 (Case 2) against the value of 1.50 for the case without the spur dike. Maximum velocity in the separation zone is $\bar{U}^* = -0.56$ (Case 2).

Variation of $\bar{u}^*$ along the width at three different locations ($s^* = 0.375$, 0.540, and 0.750) and two different elevations are presented in Fig. 4. Near the spur dike, $\bar{u}^*$ at lower elevation is higher compared to that at higher elevation [Fig. 4(a)]. Dey and Barbhuiya (2005); Duan (2009); and Koken and Constantinescu (2008) also reported such a flow pattern in the vertical direction for a spur dike

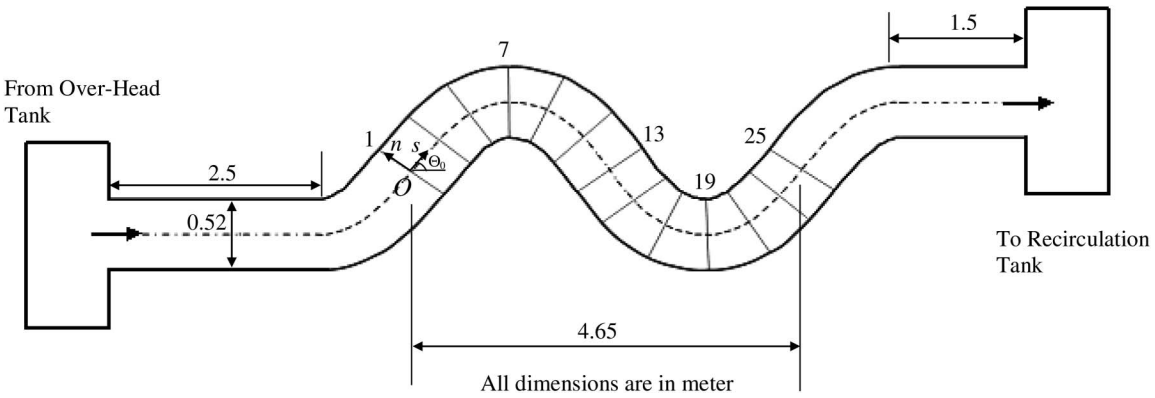

Fig. 2. Experimental setup

J. Hydraul. Eng., 2012, 138(10): 897-901

Table 2. Summary of Results

		Given conditions				Measured quantities							
		Spur dyke location						L_1^*		L_2^*		W_{max}^*	
Case	Objective	Bank	s^*	b (m)	U_{rep} (m/s)	Maximum U^*	U^* near the tip of spur dyke	$z^* = 0.5$	$z^* = 0.167$	$z^* = 0.5$	$z^* = 0.167$	$z^* = 0.5$	$z^* = 0.167$
1	Effect of location of spur dyke on right bank	Right	0.125	0.160	0.225	1.95	1.95	11.56	11.13	3.49	3.46	1.44	1.04
2		Right (apex 1)	0.250	0.160	0.225	2.26	2.10	20.00	20.25	3.75	3.75	2.06	1.50
3		Right	0.375	0.160	0.225	1.85	1.34	13.56	14.00	2.16	2.03	1.54	1.23
4		Right (crossover)	0.500	0.160	0.225	1.84	1.21	11.63	11.13	3.53	3.50	1.67	1.25
5		Right	0.675	0.160	0.225	1.70	1.16	7.44	7.31	1.84	1.88	1.37	1.20
6	Effect of location of spur dyke on left bank	Left (apex 1)	0.250	0.160	0.225	1.81	1.08	4.75	5.15	1.36	1.33	1.13	1.00
7		Left	0.375	0.160	0.225	1.62	1.20	5.69	6.00	1.38	1.34	1.25	1.13
8		Left (crossover)	0.500	0.160	0.225	1.86	1.55	7.63	6.44	1.25	1.25	1.33	1.13
9	Effect of spur dyke length when spur dyke is on right bank	Right	0.250	0.135	0.225	2.05	2.00	22.81		5.93		1.93	
10			0.250	0.110	0.225	1.98	1.93	20.82		5.45		2.00	
11			0.500	0.135	0.225	1.62	1.01	10.74		4.19		1.70	
12			0.500	0.110	0.225	1.54	0.96	11.09		5.14		1.91	
13	Effect of spur dyke length when spur dyke is on left bank	Left	0.250	0.135	0.225	1.58	1.01	5.19		1.59		1.26	
14			0.250	0.110	0.225	1.54	0.94	6.09		1.95		1.36	
15			0.500	0.135	0.225	1.72	1.60	7.19		1.48		1.33	
16			0.500	0.110	0.225	1.62	1.49	7.64		1.82		1.47	
17	Effect of inflow Froude number when spur dyke is on right bank	Right	0.250	0.160	0.141	2.20	2.00	19.25		3.75		2.06	
18			0.250	0.160	0.281	2.31	2.05	19.38		3.75		2.06	
19			0.500	0.160	0.141	1.77	1.14	11.88		3.53		1.63	
20			0.500	0.160	0.281	1.86	1.25	11.00		3.53		1.63	
21	Effect of inflow Froude number when spur dyke is on left bank	Left	0.250	0.160	0.141	1.72	0.98	4.88		1.36		1.13	
22			0.250	0.160	0.281	1.77	1.04	3.99		1.36		1.13	
23			0.500	0.160	0.141	1.75	1.49	7.88		1.25		1.31	
24			0.500	0.160	0.281	1.88	1.63	7.50		1.44		1.33	

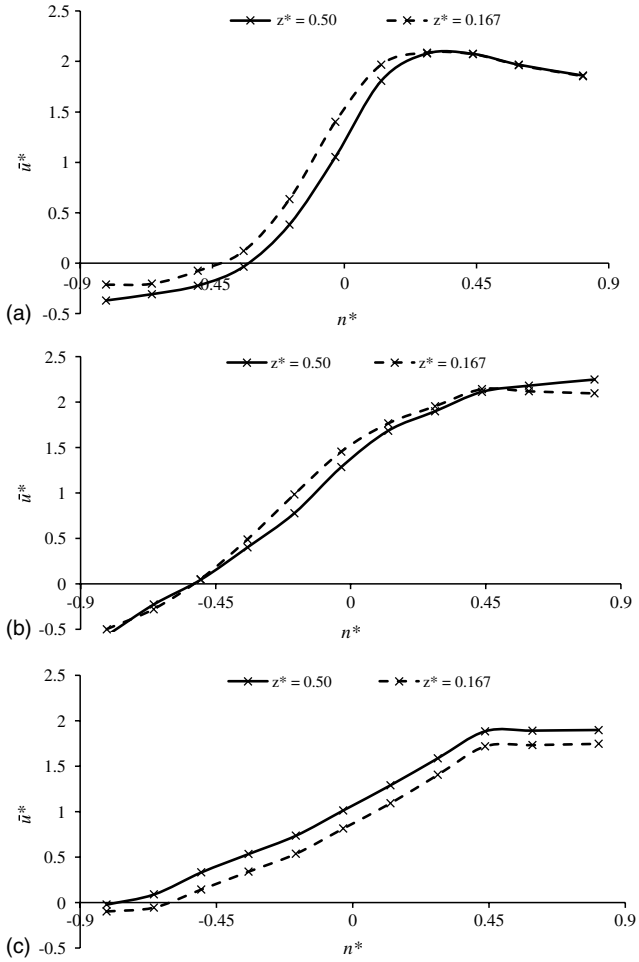

Fig. 4. Variation of longitudinal velocity along width (Case 2): (a) $s^* = 0.375$; (b) $s^* = 0.541$; (c) $s^* = 0.75$

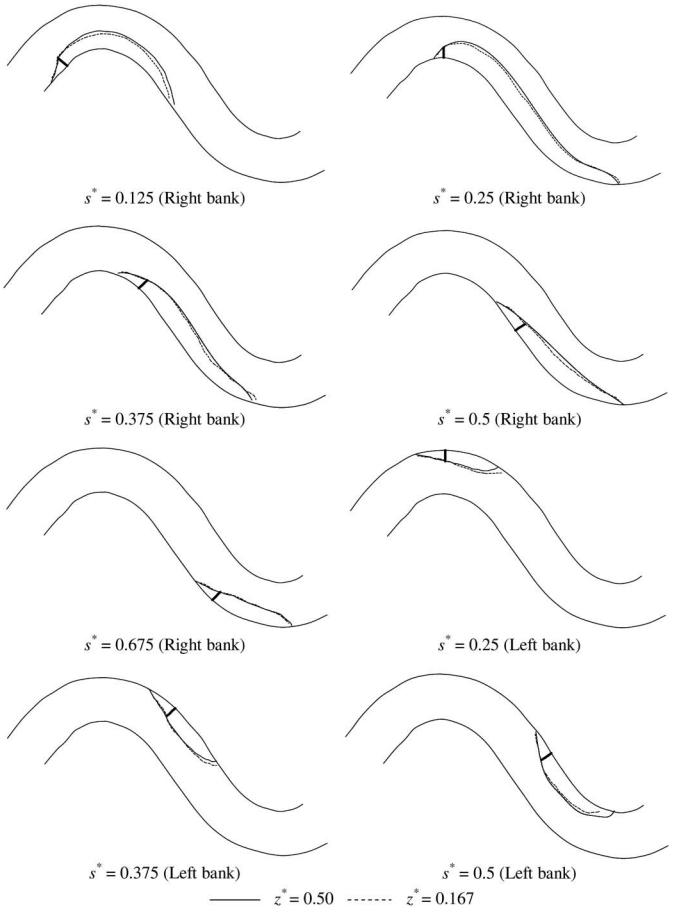

Fig. 5. Effect of spur dyke location on flow separation

in a straight channel. At $s^* = 0.541$, $\bar{u}^*$ at both elevations is similar [Fig. 4(b)]. Further downstream at $s^* = 0.750$, $\bar{u}^*$ at higher elevation is higher compared to that at lower elevation [Fig. 4(c)].

Flow Separation Zone

The variation of the longitudinal velocity, $\bar{u}^*$, along the width is used to find the boundary of the downstream separation zone. It may be defined such that total discharge in the separation zone is zero. End of the separation zone is marked where a nonnegative value of $\bar{u}$ is observed. The variable W^*_{max} is measured as the maximum width of separation zone, and L^*_2 is the distance of this section from the spur dike. Results for L^*_1, L^*_2, and W^*_{max} for all cases considered are presented in Table 2. Due to its insignificant size, the upstream flow separation zone is not presented here. The length and width of the separation zone due to various locations of the spur dike depend on the spur dike location (Fig. 5). The variables L^*_1 and W^*_{max} are observed in the range of 4.0–22.8 and 1.0–2.1, respectively. It may be recalled that corresponding values in the case of a spur dike in a straight channel were 12.0–14.0 and 1.8, respectively (Table 1). The separation zones at the middle layer for three different spur dike lengths at four different locations are presented in Table 2 (Cases 8–16). Variation of L^*_1 and W^*_{max} with CR depends on the location of the spur dike. When the spur dike is located on a right bank at $s^* = 0.25$, L^*_1 decreases by increasing CR. This may be explained by the flow pattern in the channel without a spur dike. In the downstream of the apex, flow shifts toward the outer bank. For the second apex the outer bank is with the spur dike and thus L^*_1 is limited up to the second apex. For each location, W^*_{max} is maximum for CR = 0.25. For all three spur dike lengths, L_2 is almost constant. The separation zone for three different values of F (H_{rep} remaining constant), i.e., F = 0.14, 0.23, and 0.28, and four locations at $z^* = 0.5$ are presented in Table 2. It is observed that the upstream separation zone is not affected by inflow F. However, the length and width of the downstream separation zone are both marginally affected by F.

Conclusions

An experimental study was conducted in a rigid bed meandering channel to find the flow field due to various locations of the spur dike. The main conclusions of the present study are:

1. The velocity amplification is maximum when the spur dike is located on the inner bank of the apex section.
2. The separation zone parameters, length, maximum width, and location of maximum width, depend on the location of the spur dike as given in Table 2.
3. The maximum and the minimum nondimensional downstream flow separation length is 22.8 and 4.0, respectively. Similarly, maximum and minimum nondimensional width of the downstream separation zone is 2.1 and 1.1.
4. Contraction ratio affects the separation zone when the spur dike is located on the inner bank of the apex.

J. Hydraul. Eng., 2012, 138(10): 897-901

5. Inflow Froude number has a small effect on separation zone.

Notation

The following symbols are used in this paper:

B = half width of the channel;
b = spur dyke length;
F = inflow Froude number;
H_{rep} = representative flow depth measured at $s = -2.55$ m and $n = 0.0$;
h = flow depth;
L = meander length measured along s;
L_1 = length of downstream separation zone;
L_2 = distance between section of maximum width of separation zone and spur dyke;
R = radius of curvature or center line radius;
s, n, z = space coordinates along longitudinal, transverse, and vertical directions, respectively;
U = resultant velocity in a horizontal plane;
U_{rep} = representative flow velocity measured at $s = -2.55$ m, $n = 0.0$, and $z = 0.06$ m;
$\bar{U}_{rep}$ = time averaged representative flow velocity;
u, v, w = instantaneous velocity in longitudinal, transverse, and vertical directions, respectively;
$\bar{u}$, $\bar{v}$, $\bar{w}$ = time averaged velocity in longitudinal, transverse, and vertical directions, respectively;
W_{max} = maximum width of separation zone from bank;
W_s = width of separation zone;
α = inclination to the downstream bank;
λ = meander wave length; and
θ, θ_0 = deflection angles at s and at $s = 0$, respectively.

Superscript

$*$ = corresponding nondimensional value.

References

Dey, S., and Barbhuiya, A. K. (2005). "Time variation of scour at abutments." *J. Hydraul. Eng.*, 131(1), 11–23.

Duan, J. G. (2009). "Mean flow and turbulence around a laboratory spur dike." *J. Hydraul. Eng.*, 135(10), 803–811.

Ettema, R., and Muste, M. (2004). "Scale effects in flume experiments on flow around a spur dike in flatbed channel." *J. Hydraul. Eng.*, 130(7), 635–646.

Giri, S., Shimizu, Y., and Surajate, B. (2004). "Laboratory measurement and numerical simulation of flow and turbulence in a meandering-like flume with spurs." *Flow Meas. Instrum.*, 15(5–6), 301–309.

Koken, M. (2011). "Coherent structures around isolated spur dykes at various approach flow angles." *J. Hydraul. Res.*, 49(6), 736–743.

Koken, M., and Constantinescu, G. (2008). "An investigation of the flow and scour mechanisms around isolated spur dikes in a shallow open channel: 2. Conditions corresponding to the final stages of the erosion and deposition process." *Water Resour. Res.*, 44, W08407.

Molls, T. R., and Chaudhry, M. H. (1995). "A depth-averaged open-channel flow model." *J. Hydraul. Eng.*, 121(6), 453–465.

Nagata, N., Hosoda, T., Nakata, T., and Muramoto, Y. (2005). "Three dimensional numerical model for flow and bed deformation around river hydraulic structures." *J. Hydraul. Eng.*, 131(12), 1074–1087.

Nortek. (2011). "Vectrino." ⟨http://www.nortek-as.com/lib/data-sheets/data sheet-vectrino-lab⟩ (Oct. 10, 2009).

Ouillon, S., and Dartus, D. (1997). "Three-dimensional computation of flow around groyne." *J. Hydraul. Eng.*, 123(11), 962–970.

Rajaratnam, N., and Nwachukwa, B. A. (1983). "Flow near groin-like structures." *J. Hydraul. Eng.*, 109(3), 463–480.

Sharma, K., and Mohapatra, P. K. (2009). "Numerical study of reattachment length for flow past spur dyke in a meandering channel." *Proc., River Hydraulics 2009*, Indian Society of Hydraulics, Khadakwasla, India, 124–132.

Tingsanchali, T., and Mahesawaran, S. (1990). "2D depth-averaged flow computation near groyne." *J. Hydraul. Eng.*, 116(1), 71–86.

Wahl, T. L. (2003). "Discussion of despiking acoustic Doppler velocimeter data." *J. Hydraul. Eng.*, 129(6), 484–487.